

swirl acts to reduce axial velocity on and near the core axis. This effect is reversed as radial distance from the axis increases, with a further, but only slight, reversal occurring toward the outer region of the core. It is of interest to investigate whether this modification will be sufficient to shift the axial velocity maximum off the core axis for a large enough degree of swirl in the jet case. This requires  $\partial^2 w / \partial r^2|_{r=0} > 0$ ,  $w|_{r=0} > W_0$  which, from Eq. (29) may be found to imply  $Sl_n(W_0 z / \nu) > 512\pi/15$ ,  $Sl_n(W_0 z / \nu) < 512\pi/5$ , respectively. However, since  $S_{\max} \approx 1$  and  $S \sim z^{-2}$  it is difficult to see how the former condition can ever be met. On the other hand, the solution indicates that the far field of the momentumless jet ( $F=0$ ) exhibits an axial velocity profile with maximum velocity off the centerline.

### Acknowledgment

The author would like to thank Prof. B. R. Morton for his help and advice regarding this work.

### References

- <sup>1</sup>Batchelor, G. K., "Axial Flow in Trailing Line Vortices," *Journal of Fluid Mechanics*, Vol. 20, 1964, pp. 645-658.
- <sup>2</sup>Morton, B. R., "The Strength of Vortex and Swirling Core Flows," *Journal of Fluid Mechanics*, Vol. 38, 1969, pp. 315-333.
- <sup>3</sup>Newman, B. G., "Flow in a Viscous Trailing Vortex," *The Aeronautical Quarterly*, Vol. 10, 1959, pp. 149-162.
- <sup>4</sup>Berger, S. A., "The Incompressible Laminar Axisymmetric for Wake," *Journal of Mathematics and Physics*, Vol. 47, 1968, pp. 292-309.

## A Local Similarity Solution for the Viscous Boundary-Layer Flow Longitudinal to a Cylinder

Richard E. Sayles\*  
University of Maine, Orono, Maine

### Nomenclature

- $a$  = radius of the cylinder  
 $c$  =  $a(w_0/\nu z)^{1/2}$  = curvature parameter  
 $C_f$  =  $2\tau_w/\rho w_0^2$  = dimensionless wall shear stress  
 $f$  =  $w/w_0$  = dimensionless axial velocity  
 $r, z$  = radial and axial coordinates, respectively  
 $Re_z$  =  $w_0 z/\nu$  = Reynolds number  
 $s$  =  $\nu z/w_0 a^2$  = dimensionless axial coordinate  
 $u, w$  = radial and axial velocity components, respectively  
 $y$  =  $r - a$  = distance above the cylinder surface  
 $\eta$  =  $y(w_0/\nu z)^{1/2}$  = Blasius similarity variable  
 $\nu$  = kinematic viscosity  
 $\rho$  = density  
 $\tau$  = shear stress

### Subscripts

- $0$  = reference condition  
 $w$  = conditions at the cylinder surface

### Introduction

THE boundary-layer flow longitudinal to a cylinder is complicated by the transverse curvature of the surface,

which precludes the possibility of obtaining a similarity solution to the governing boundary-layer equations. Since a similarity solution cannot be found, one naturally wonders whether a transformation of the boundary-layer equations exists that will minimize the streamwise variation of the velocity profiles. If such a transformation exists, the boundary-layer equations may, with some error resulting, be solved to obtain the local velocity profile and local surface shear stress without the necessity of accounting for the streamwise history of the boundary-layer flow.

The most accurate analysis of the problem of a uniform flow longitudinal to a semi-infinite, constant-radius cylinder appears to be that of Sparrow et al.,<sup>1</sup> in which a coordinate transformation was employed that was first suggested by Seban and Bond.<sup>2</sup> This coordinate transformation results in a dimensionless boundary-layer thickness that varies by a factor of 15 over the solution domain which, therefore, precludes the possibility of obtaining an accurate local similarity solution to the transformed equations. Presented in this Note is a coordinate transformation of the boundary-layer equations that substantially reduces the streamwise variation of the velocity profiles and the dimensionless boundary-layer thickness. The transformed equations can then be solved as ordinary differential equations to obtain the local velocity profile and local surface shear stress with an error or 2-5% resulting in the surface shear stress.

### Analysis

The governing incompressible boundary-layer equations, written in cylindrical coordinates, are

$$\frac{\partial}{\partial r}(ru) + \frac{\partial}{\partial z}(rw) = 0 \quad (1)$$

and

$$u \frac{\partial w}{\partial r} + w \frac{\partial w}{\partial z} = \nu \left( \frac{1}{r} \frac{\partial w}{\partial r} + \frac{\partial^2 w}{\partial r^2} \right) \quad (2)$$

The first term on the right-hand side of Eq. (2) introduces the transverse curvature effect that precludes the possibility of obtaining a similarity solution for this boundary-layer flow. Since a similarity solution does not exist, a dimensionless axial velocity component is defined as

$$f(\eta, s) = w/w_0$$

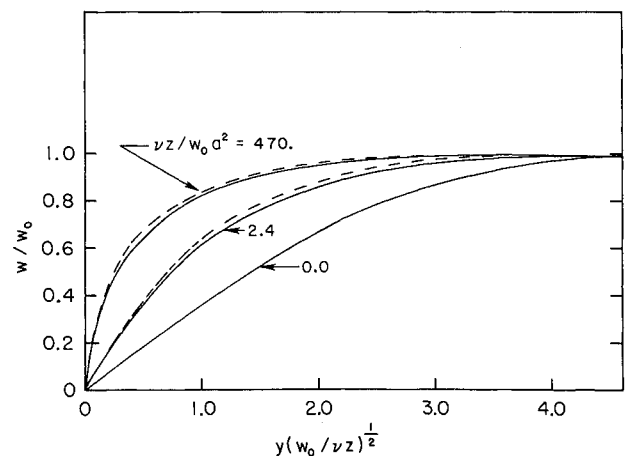


Fig. 1 Velocity profiles at various axial distances for the flow longitudinal to a constant-radius cylinder: (—) difference-differential solutions, (---) local similarity solution.

Received April 9, 1983; revision received Aug. 8, 1983. Copyright © American Institute of Aeronautics and Astronautics, Inc., 1983. All rights reserved.

\*Assistant Professor of Mechanical Engineering, Department of Mechanical Engineering.

**Table 1 Dimensionless wall shear stress for the flow longitudinal to a stationary, constant-radius cylinder ( $C_f Re_z^{1/2}$ )**

$s = \nu z / w_0 a^2$	Ref. 5	Ref. 1 <sup>a</sup>	Ref. 6	Difference-differential	Local similarity
0.01	0.6881	0.795	0.7931	0.7945	0.8145
0.05	0.8271	0.934	0.9453	0.9331	0.9675
0.10	0.9172	1.02	1.075	1.027	1.0690
0.50	1.248	1.36	2.139	1.380	1.4440
1.00	1.468	1.63	3.991	1.614	1.6910
5.00	2.273	2.44	33.55	2.461	2.5740
10.00	2.807	3.04	—	3.024	3.1590
50.00	4.788	5.12	—	5.108	5.2910
100.00	6.121	6.50	—	6.512	6.7220
500.00	11.13	—	—	11.75	12.0400
1000.00	14.56	—	—	15.33	15.6700

<sup>a</sup> Interpolated from graphical results.

where  $w_0$  is a reference velocity. The dimensionless independent variables  $\eta$  and  $s$  are defined as

$$\eta = y(w_0/\nu z)^{1/2}, \quad s = \nu z / w_0 a^2$$

where  $y = r - a$  is the normal distance above the cylindrical surface. The axial variation of the function  $f$  is accounted for with its dependence on  $s$ , and the variable  $\eta$  is the Blasius similarity variable for two-dimensional flat-plate boundary-layer flow.

From Eq. (1), the radial velocity component can be expressed as

$$u = -\frac{1}{r} \int_0^r \frac{\partial}{\partial z} (rw) dr$$

Substitution of this expression into Eq. (2) and using the dimensionless variables defined above, the conservation of momentum equation becomes

$$f'' = \frac{-f'}{2(1+\eta/c)} \int_0^\eta f d\eta - \frac{f'}{(\eta+c)} \left[ 1 + \int_0^\eta \eta f d\eta \right] + s \left[ f \frac{\partial f}{\partial s} - \frac{f'}{(\eta+c)} \frac{\partial}{\partial s} \int_0^\eta \eta f d\eta - \frac{f'}{(1+\eta/c)} \frac{\partial}{\partial s} \int_0^\eta f d\eta \right] \quad (3)$$

where the primes refer to differentiation with respect to  $\eta$ . Although this transformation leads to a more complicated form of the boundary-layer equation than that resulting from the transformation of Seban and Bond,<sup>2</sup> the equation above is favorable for several reasons. The effect of transverse curvature is clearly evident in the terms containing the parameter  $c$ . Also, the Blasius boundary-layer equation is easily obtained from Eq. (3) by letting the parameter  $c$  approach infinity and neglecting the  $\partial/\partial s$  terms, which assures that the initial development of the boundary layer will be the same as that which occurs on a two-dimensional plane surface. Therefore, Eq. (3) is applicable to either plane boundary-layer flows or boundary-layer flows with transverse curvature effects. Furthermore, as will be shown, the use of the Blasius similarity variable substantially reduces the streamwise variation of the velocity profiles.

### Solution Method

The difference-differential solution method was employed to solve Eq. (3). The streamwise derivatives were approximated using a three-point-backward difference formula that requires a knowledge of two upstream velocity profiles. The initial two profiles were generated by neglecting the  $\partial/\partial s$  terms in Eq. (3), which are quite small near the leading edge, since the departure from the Blasius plane flow solution is small in this region. Once the streamwise derivatives have

been estimated, Eq. (3) becomes an ordinary differential equation in  $\eta$  that can be solved to obtain the local velocity profile and the local shear stress. A trial-and-error procedure must be used to solve the ordinary differential equation since the value of  $f'(0,s)$  is unknown. Hartree and Womersley<sup>3</sup> introduced this solution technique and Smith and Clutter<sup>4</sup> applied it to two-dimensional plane boundary-layer flows with arbitrary pressure gradients.

### Results

For comparative purposes, prime consideration will be given to the wall shear stress, which may be expressed in a dimensionless fashion as

$$C_f Re_z^{1/2} = 2f'(0,s)$$

where

$$C_f = 2\tau_w / \rho w_0^2 \quad \text{and} \quad Re_z = w_0 z / \nu$$

Equation (3) was solved subject to the following boundary conditions:

$$f(0,s) = 0.0 \quad \text{and} \quad f(\infty,s) = 1.0$$

which corresponds to the axial flow of a uniform stream over a stationary, constant-radius cylinder. The numerical results for this flow are presented in Table 1 along with the momentum integral results of Glauert and Lighthill,<sup>5</sup> the local nonsimilarity results of Sparrow, Quack, and Boerner,<sup>1</sup> and the series solution results of Wanous and Sparrow.<sup>6</sup> Also presented in Table 1 are local similarity results obtained by setting the streamwise derivatives to zero in Eq. (3).

The difference-differential results compare quite favorably with the local nonsimilarity results of Sparrow, Quack, and Boerner. The error in the wall shear stress incurred by invoking the local similarity approximation is 2-5% over the entire solution domain. Typical velocity profiles from both the difference-differential and local similarity solutions are presented in Fig. 1, from which it is seen that the streamwise variation of the boundary-layer thickness is only 15-25%. If the transformation of Seban and Bond had been used, the dimensionless boundary-layer thickness would have increased by a factor of 15, as was reported in Ref. 1.

### Conclusions

It has been shown that by transforming the boundary-layer equations, written in cylindrical coordinates, using the Blasius similarity variable substantially reduces the streamwise variation of the velocity profiles compared with that resulting when the Seban and Bond transformation is employed. The streamwise variation of the dimensionless boundary-layer thickness was only 15-25% over the entire solution domain

for the boundary-layer flow longitudinal to a stationary, constant-radius cylinder. For this flow, the wall shear stress obtained from a local similarity solution of the boundary-layer equations is within 2-5% of the difference-differential solution.

### References

- <sup>1</sup>Sparrow, E. M., Quack, H. and Boerner, C. J., "Local Non-similarity Boundary-Layer Solutions," *AIAA Journal*, Vol. 8, Nov. 1970, pp. 1936-1942.
- <sup>2</sup>Seban, R. A. and Bond, R., "Skin Friction and Heat Transfer Characteristics of a Laminar Boundary Layer on a Cylinder in Axial Incompressible Flow," *Journal of the Aeronautical Sciences*, Vol. 8, Oct. 1951, pp. 671-675.
- <sup>3</sup>Hartree, D. R. and Womersley, J. R., "A Method for the Numerical or Mechanical Solution of Certain Types of Partial Differential Equations," *Proceedings of the Royal Society of London*, Ser. A, Vol. 101, Aug. 1937, pp. 353-366.
- <sup>4</sup>Smith, A. M. O. and Clutter, D. W., "Solution of the Incompressible Laminar Boundary-Layer Equations," *AIAA Journal*, Vol. 1, Sept. 1963, pp. 2062-2071.
- <sup>5</sup>Glauert, M. B. and Lighthill, M. J., "The Axisymmetric Boundary Layer on a Long Cylinder," *Proceedings of the Royal Society of London*, Ser. A, Vol. 230, No. 1181, June 1966, pp. 188-203.
- <sup>6</sup>Wanous, D. J. and Sparrow, E. M., "Longitudinal Flow Over a Circular Cylinder with Surface Mass Transfer," *AIAA Journal*, Vol. 3, Jan. 1965, pp. 147-149.

## Closed-Form Model for Three-Dimensional Vacuum Plumes from a Scarfed Nozzle

G. L. Romine\* and J. A. Noble†

Martin Marietta Corporation, Denver, Colorado

### Nomenclature

- $C_F$  = axial-component thrust coefficient  
 $E$  = coefficient in density model  
 $F$  = axial-component thrust parameter  
 $M$  = Mach number  
 $N$  = exponent in density model  
 $P$  = pressure  
 $R$  = radius from nominal exit plane to point in the plume  
 $T$  = temperature  
 $V$  = velocity  
 $\alpha$  = thrust vector angle from nozzle axis  
 $\gamma$  = ratio of specific heats  
 $\zeta$  = polar/azimuthal function used in density model  
 $\theta$  = azimuthal angle from nozzle axis  
 $\nu$  = Prandtl-Meyer angle  
 $\rho$  = density  
 $\sigma$  = scarf angle of exit plane from axis normal  
 $\phi$  = polar angle about axis, from highest area ratio

### Superscripts

- ( )<sup>\*</sup> = throat condition

### Subscripts

- ex = nozzle exit condition  
 $m$  = condition at expansion to  $T = 0$  deg  
 $c$  = chamber conditions  
 $B$  = boundary  
 $N$  = nozzle

Received May 5, 1983. Copyright © American Institute of Aeronautics and Astronautics, Inc., 1983. All rights reserved.

\*Sr. Staff Engineer. Member AIAA.

†Engineer. Member AIAA.

**P**LUME impingement by attitude control system (ACS) exhausts during deployment or retrieval maneuvers in space can cause serious dispersions to payload trajectories. In order to quantify these ACS plume effects, a reliable model is desired for the plume flowfield. If the ACS nozzle centerline is not perpendicular to the vehicle surface, the exit plane is scarfed or tilted relative to the nozzle axis. The exit Mach number and expansion into the plume will vary peripherally depending upon the local area ratio. Consequently, scarfed nozzle plumes are three dimensional and difficult to quantify. Prior attempts to bound these flows consisted of a patchwork of axisymmetric calculations for each quadrant, and an extrapolation across the axis and between quadrants.

For ease in computation, a closed-form analytical model is desired to simulate the three-dimensional vacuum plume from a scarfed nozzle. A second requirement of the model is that, in the limit of zero scarf angle, the model describes a vacuum plume from a conventional nozzle and takes into account the plume size as a function of maximum turning at the exit. A further requirement for the model is that the exponent for the angular density dependence follow the two-dimensional hypersonic approximation of  $2/\gamma - 1$  shown by Boynton<sup>1</sup> to apply to the leading edge of the plume expansion. Although several models are available in the literature for axisymmetric vacuum plumes, none meet the last two requirements directly for the scarfed nozzle plume modifications. The model of Karydas and Kato<sup>2</sup> assumes a fixed 90-deg plume boundary angle, but was the most adaptable for the present requirements and was used as a departure point.

The standard vacuum plume assumptions are made; i.e., the flow can be represented by a source, the density decays with the inverse distance squared, the gas expands to its limiting velocity, the plume is in a vacuum with no boundary shocks, and that the radial density distribution may be described by a single function. The resulting expression for density is

$$\rho = \frac{E}{2} \rho^* \frac{V^*}{V_m} \left( \frac{R^*}{R} \right)^2 \cos^N \zeta \quad (1)$$

where the constants  $E$  and  $N$  are to be specified by mass and momentum balances shown below, and the parameter  $\zeta$  is a three-dimensional plume angle from the centerline which is normalized with its local maximum.

The scarfed nozzle plume description must satisfy certain physical boundary conditions. These are as follows.

- 1) The plume flow will ultimately adjust to the scarfed exit conditions such that the angle where the maximum density occurs is along the thrust vector  $\alpha$ . Consequently, the in-

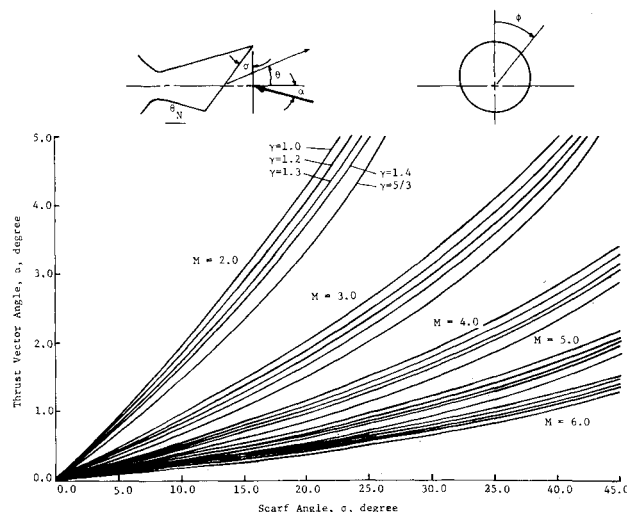


Fig. 1 Thrust vector offset due to scarf angle ( $\theta_N = 10$  deg).